Applied Engineering Letters Vol.9, No.2, 94-104 (2024) e-ISSN: 2466-4847

# THERMAL SOURCE EFFECT ON THE NATURAL CONVECTION OF A NANOFLUID WITHIN A TRIANGULAR CAVITY

UDC:532:536.2
Original scientific paper https://doi.org/10.46793/aeletters.2024.9.2.4

**Mohamed Amine Belmiloud [1*], Said Mekroussi[1], Bendaoud Mebarek[2], Hadj Madani Meghazi[2], Momen S.M. Saleh[1]**

[1]Research Laboratory of Industrial Technologies, Department of Mechanical Engineering, University of Tiaret, 14000, Algeria
[2]Research Laboratory of Artificial Intelligence and Systems (LRIAS), University of Tiaret, Algeria

**Abstract:**
Natural convection is numerically studied in a triangular cavity whose inclined walls that is isothermal at temperature $T_C$, while its base is thermally insulated. The cavity contains a hot isothermal cylindrical heat source $T_H$ of diameter $D$. In this study, we used the nanofluid (water + $TiO_2$). The nanoparticle volume fraction is varied within the range $0.01 \le \phi \le 0.05$, and the Rayleigh number is set between $10^3$ and $10^6$. The main objective of this study is to explore the impact of nanoparticle concentration, Rayleigh number (*Ra*), and heat source position (*h*) on the enhancement of convective thermal transfer. The simulation results show that thermal exchange improves with increasing *Ra*, heat source diameter, and nanoparticle volume fraction ($\phi$).

**ARTICLE HISTORY**
Received: 28 April 2024
Revised: 19 June 2024
Accepted: 27 June 2024
Published: 30 June 2024

**KEYWORDS**
Natural convection, Triangular cavity, Thermal exchange, Nanofluids, $TiO_2$, Modelling

## 1. INTRODUCTION

The enhancement of thermal exchange has been the focus of numerous research studies. Various authors have conducted theoretical, numerical, and experimental investigations to describe convection phenomena. These studies are particularly relevant due to their applications in diverse industries, such as cooling electronic equipment, thermal devices, nuclear power plants, and solar collectors. Some researchers have shown particular interest in enhancing thermal exchange using nanofluids [1-3]; studying nanofluids in various objects, such as a cylinder or a circular tube, leads to improved heat transfer by increasing the particle size concentration [4-5]. Some researchers also used nanofluids in square [6], rectangular [7] and *L* -shaped triangular cavities [8] in order to improve thermal performance, which produced remarkable results compared to using regular fluids. In this context, researchers carefully analyzed nanoparticles in order to measure thermal conductivity, and they found that using this type in studies gives better conductivity than ordinary liquids [9-11]. Their findings demonstrated the efficiency of nanofluids compared to base fluids (water) in terms of thermal exchange. Ouyahia et *al.* [12] investigated numerically the thermo-hydraulic characteristics of water-$TiO_2$ nanofluid in an isosceles-triangular cavity. They presented flow and thermal field mappings, along with the average Nusselt number inside the cavity. Their findings showed an intensification of thermal and flow fields with the rise of Rayleigh number. Natural convection heat transfer of a hybrid nanofluid in a permeable quadrantal enclosure with heat generation was presented by Khan et al [13]. Their findings revealed. Their than the average Nusselt number depends on $\phi$, exhibiting an increase with rising $\phi$. Ghasemi and Aminossadati [14] studied the nanoparticles' Brownian motion inside a triangular-shaped enclosure. For all considered volume fractions, they found an increase in the thermal exchange rate vs. Rayleigh number. Also, the heat source location has a considerable influence on the thermal exchange rate.

*CONTACT: Mohamed Amine Belmiloud, e-mail: belmiloud_amine@yahoo.fr

A computational study of convection in a rectangular cavity was presented by Boudjeniba et al. [15], The results obtained show that the fluid flow starts as stationary, transitions through periodic flow after a supercritical Hopf bifurcation, and then becomes quasi-periodic at two different frequencies, ultimately leading to chaotic convection in both pure fluid and nanofluid. Oztop and Abu-Nada [16] examined convection in partially heated cavities, highlighting the effects of Ra, heating element length and location, aspect ratio, and fluid concentration on hydrothermal characteristics. Vedavathi et al. [17] investigated natural convection flow in semi-trapezoidal porous enclosure filled with alumina-water nanofluid using Tiwari and Das' nanofluid model. Their results indicated that an increase in the Rayleigh number leads to an increase in heat transfer, where one can find a reduction of convective heat transfer with $\phi$. Many researchers have studied the effect of many parameters such as *Ra* number, the volume fraction of nanofluid, and *Ri* number in their research. From their results, it was discovered that the *Ra* number and *Ri* number have significant values in the *Nu* number [18-22]. Furthermore, magnetohydrodynamic (MHD) analyzes of convection by nanofluids in complex geometries have been the subject of several researchers [23-25]. The results indicate that corrugated geometry and magnetic fields play a crucial role in controlling heat transfer rates, entropy generation and flow behaviour.

This work aims to evaluate the influence of physical factors (Rayleigh number and nanoparticle concentration) and geometric parameters, such as the size and location of the thermal source, on the dynamic and thermal characteristics of a nanofluid (water-$TiO_2$) confined within a triangular cavity.

## 2. MATHEMATICAL FORMULATION

The problem considered in a triangular cavity is presented in Fig. 1. The dimensions of the cavity are its length, *L*, and its height *H*, such that *L=H*. The inclined walls of the cavity are cold isothermal *TC*, while its base is thermally insulated. On the other hand, the cavity is provided with a hot isothermal cylindrical heat source *TH* of diameter *D*. The latter is moved vertically by the height *h*. In this research the nanofluid water + $TiO_2$ and the volume fraction of the nanoparticles is taken in the range $0 \le \phi \le 0.05$. The Rayleigh number between $10^3$ and $10^6$.

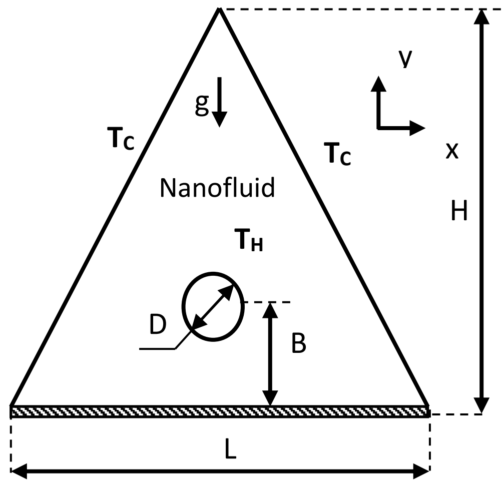


**Fig. 1.** Dimensions of the cavity

The physico-thermal characteristics of the working fluids are given by the correlations of Khanafer et al. [26], as summarized in Table 1.

**Table 1.** Physico-thermal characteristics of the working fluids at the temperature T = 25°C

| | Cp (J/kgK) | ρ (kg/m³) | K (W/mK) | β(1/ K)×10⁻⁵ |
|---|---|---|---|---|
| Water | 4179 | 997.1 | 0.613 | 21 |
| $TiO_2$ | 686.2 | 4250 | 8.9538 | 0.9 |

The nanofluid density is given by the following expression:

$$\rho_{nf} = (1-\phi)\rho_f + \phi\rho_{np} \tag{1}$$

The specific heat of nanofluid is given by:

$$Cp_{nf} = \frac{(1-\phi)(\rho\cdot Cp)_f + \phi(\rho\cdot Cp)_{np}}{(1-\phi)\rho_f + \phi\cdot\rho_{np}} \tag{2}$$

as well as by the following relation:

$$Cp_{nf} = (1-\phi)Cp_f + \phi Cp_{np} \tag{3}$$

The viscosity model used is based on volume concentration where the viscosity of nanofluids for spherical solid particles less than 1% by volume is determined by the following equation:

$$\mu_{nf} = \mu_f(1 + 2.5\phi) \tag{4}$$

or through the relationship that includes the following concentrated comments:

$$\mu_{nf} = \frac{\mu_f}{(1-\phi)^{2.5}} \tag{5}$$

Thermal conductivity can be calculated with the following relationship:

$$\frac{K_{nf}}{K_f} = \frac{K_{np} + 2K_f + 2\phi(K_{np} - K_f)}{K_{np} + 2K_f + \phi(K_{np} - K_f)} \tag{6}$$

Equations (1), (3), and (6) determine the nanofluid properties for the purposes of this research.

### 2.1 Figure Style and Format

The laminar and two-dimensional flow of the nanofluid were considered. The fluid was assumed to be incompressible and following the Boussinesq approximation. The fluid details were determined at an average temperature. The main equations following these assumptions are expressed as:

$$\frac{\partial u}{\partial x}+\frac{\partial v}{\partial y}=0 \tag{7}$$

$$\rho_{nf}\left(u\frac{\partial u}{\partial x}+v\frac{\partial u}{\partial y}\right)=-\frac{\partial p}{\partial x}+\mu_{nf}\left[\frac{\partial^2 u}{\partial x^2}+\frac{\partial^2 u}{\partial y^2}\right] \tag{8}$$

$$\rho_{nf}\left(u\frac{\partial v}{\partial x}+v\frac{\partial v}{\partial y}\right)=-\frac{\partial p}{\partial x}+\mu_{nf}\left[\frac{\partial^2 v}{\partial x^2}+\frac{\partial^2 v}{\partial y^2}\right]+\rho_{nf}.\beta_f.g(T-T_0) \tag{9}$$

In the same way, as for the momentum balance, we will introduce the energy conservation equation:

$$u\frac{\partial T}{\partial x}+v\frac{\partial T}{\partial y}=\alpha_{nf}\left[\frac{\partial^2 T}{\partial x^2}+\frac{\partial^2 T}{\partial y^2}\right] \tag{10}$$

The Nusselt number based on the diameter D is given by the relationship:

$$Nu=\frac{h_{nf}\cdot D}{K_f} \tag{11}$$

where are:
*u, v* - components of velocity, (m/s);
*x, y* - cartesian coordinates, (m);
*P* - pressure, (N/m$^2$);
$\rho$ - density, (kg /m$^3$);
$\mu$ - dynamic viscosity, (kg/ms$^2$);
$N_u$ - Nusselt number;
$\beta$ - thermal expansion coefficient, (1/K);
*T* - temperature, (K);
$\alpha$ - thermal diffusivity, (m$^2$/s).
*k* -thermal conductivity, (W/m K);
*g* - gravitational acceleration, (m/s$^2$);
*D* - diametre of source;
*H* - hot;
*C* - cold;
*av* - average.

## 3. COMPUTATIONAL PROCEDURE AND CHECKING

A finite difference approach was used to solve the main equations, which were discretized over a control volume. The SIMPLE algorithm was employed for pressure-velocity coupling. A detailed description of this technique is available in research [27]. The convergence criterion is set as:

$$\frac{|\gamma_n-\gamma_{n-1}|}{|\gamma_n|}<10^{-5} \tag{12}$$

The numerical simulation was carried out with the ANSYS Fluent commercial code. For the numerical validation of the computer code, we compare the numerical results of this study with those obtained by Arefmanesh et al. [28]. The changes in the average amounts of Nusselt number obtained at the level of the hot wall for the $TiO_2$—water and for the nanoparticle concentration $\phi$=0.02, Rayleigh number $Ra$=10$^6$, and the ratio *AR*=0.5 is practically identical to that of [28]. Namely, this study shows 13.0221, while Arefmanesh et al. [28] achieved 13.0431.

### 3.1 Domain Mesh

The key findings are highlighted in terms of thermal and flow fields, and the change in the hot-wall Nusselt number. The mesh is unstructured (121X121), it gives more accurate values in comparison with other mesh sizes. The results obtained for water - $TiO_2$ nanofluid, $Ra$=10$^6$, $\phi$=0.01 and *B*=0.5H, with this mesh (121X121), are comparable to those obtained for the mesh of (61X61), (81X81) and (101X101). The fineness of the mesh (61×61) generates maximum variations lower than 0.65% in terms of $Nu_{av}$ (Table 2). As clearly observed, there is a small difference between the results of the four meshes. This fineness is used for all subsequent calculations.

**Table 2.** Mesh effect on the results obtained for water - $TiO_2$ nanofluid, $Ra$=10$^6$, $\phi$=0.01, *B*=0.5H and for source diameter *D*=0.1 L

| Mesh | 61X61 | 81X81 | 101X101 |
|---|---|---|---|
| $Nu_{av}$ | 2.614 | 2.605 | 2.600 |
| Error (%) | 0.650 | 0.310 | 0.100 |

## 4. RESULTS AND DISCUSSION

The physical parameters involved in the considered case are the Rayleigh number (*Ra*), the particle concentration, the geometric conditions and the heat source location. The following section examines the effects of *Ra* and volume concentration $\phi$ on the fluid flow and thermal exchange behaviour. Numerical simulations were conducted for a laminar regime using water-$TiO_2$ nanofluid.

### 4.1 Stream Lines and Isothermal Lines

The flow and thermal lines for the pure water (solid line) and the pure water - $TiO_2$ nanofluid (broken line), for a Rayleigh number *Ra*=$10^5$, the source position at the height *B*=0.25H and a particle concentration $\phi$=0.05 is plotted in Fig. 2. The results demonstrate that the impact of the injected nanoparticles in the pure fluid is evident. The isothermal lines of water-$TiO_2$ overlap with those of the pure fluid at the level of the thermal source.

Fig. 3 illustrates the streamlines and the isothermal lines for a volume concentration of nanofluid $\phi$=0.01 and for a heat source of diameter *D*=0.1L positioned at the height of *B*=0.25H. It has been observed that increasing the Rayleigh number Ra leads to increased velocities in the two nanofluid recirculation cells surrounding the heat source, and that these two cells move significantly towards the top of the triangular cavity, this demonstrates that increasing the number of Rayleigh *Ra* stimulates the molecules of fluid (nanofluid) to increase the circulation velocity in the cavity. For the shape of the isothermal lines, we note that the distribution of heat provided by the source is better when the circulation velocity in the cavity is increased. In order to improve the heat transfer, the number *Ra* must be increased.

The influence of the source position (*h*) on the streamlines and thermal fields for Rayleigh number *Ra*=$10^5$ and $\phi$=0.05 is illustrated in Fig. 4. The circulation velocity in the cavity increases with the augmented distance between the thermal source and the cold walls. For the shape of the isothermal lines, we note that the distribution of heat provided by the source is better with a significant distance between the cold sides and the heat source. The source must be moved away from the walls for further enhancement of the thermal exchange.

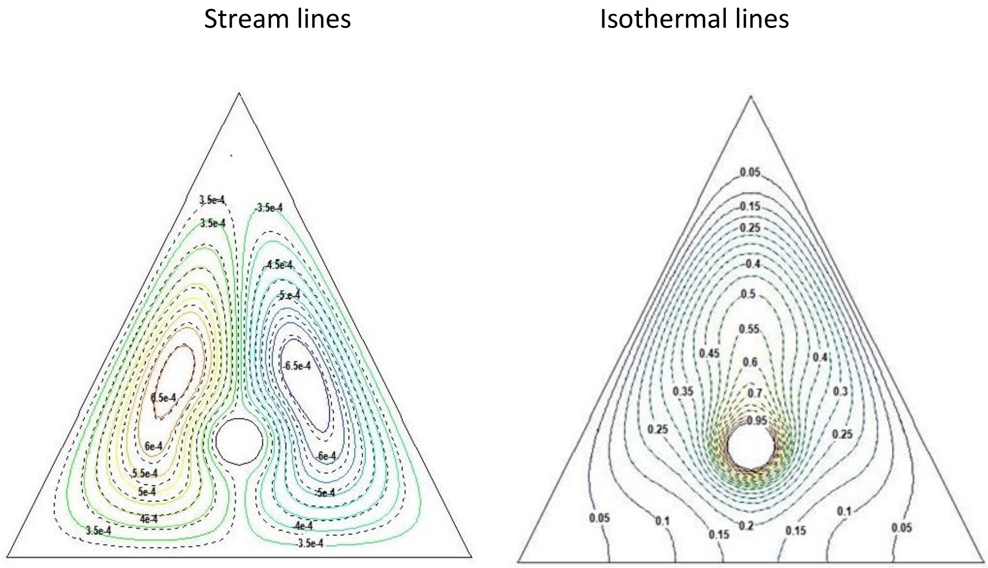


**Fig. 2.** Stream lines and isothermal lines for pure water (__), water-$TiO_2$ nanofluid (---)

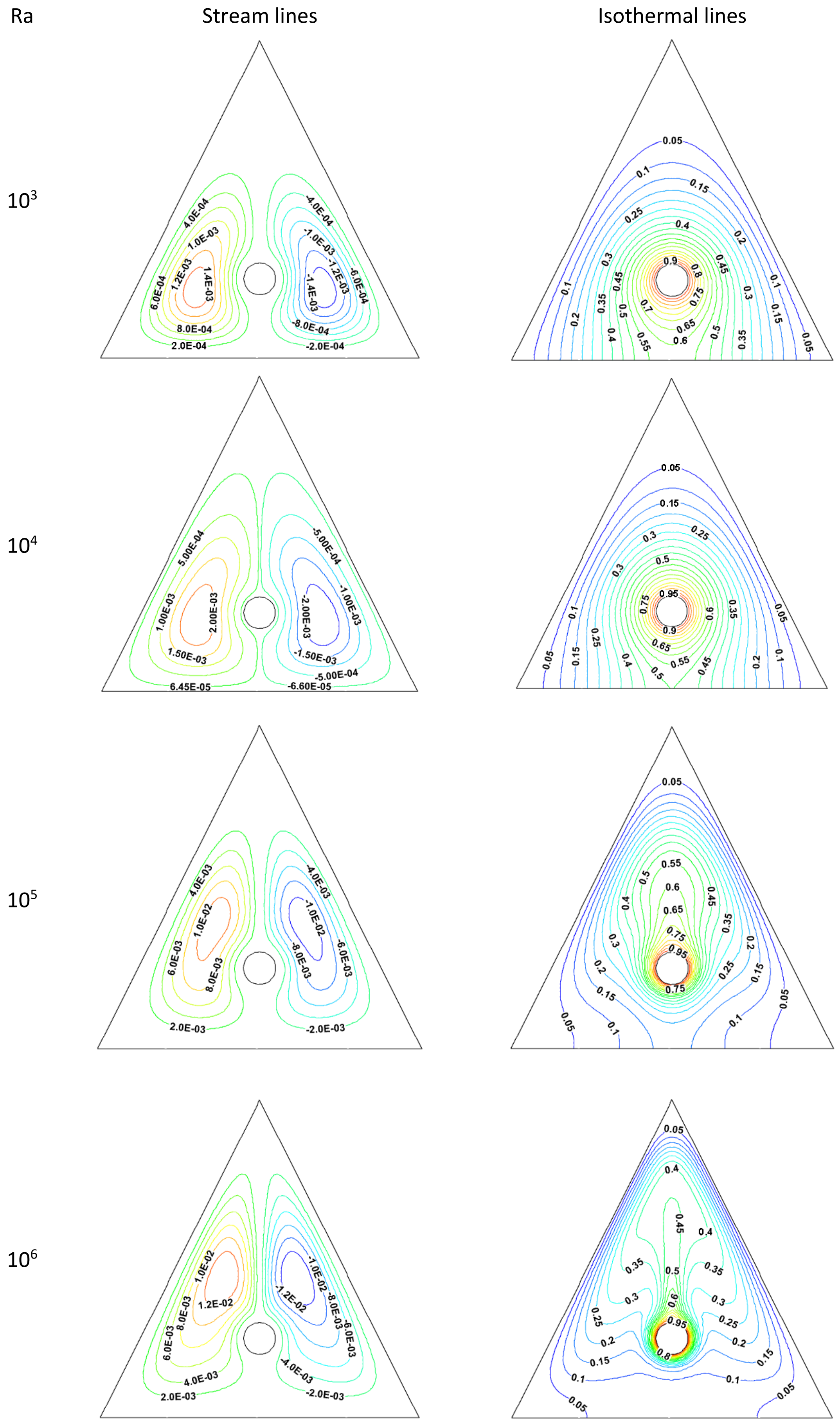


**Fig. 3.** Influence of the Rayleigh number *Ra* on stream lines and isothermal lines for *B*=0.25H and $\phi$=0.01

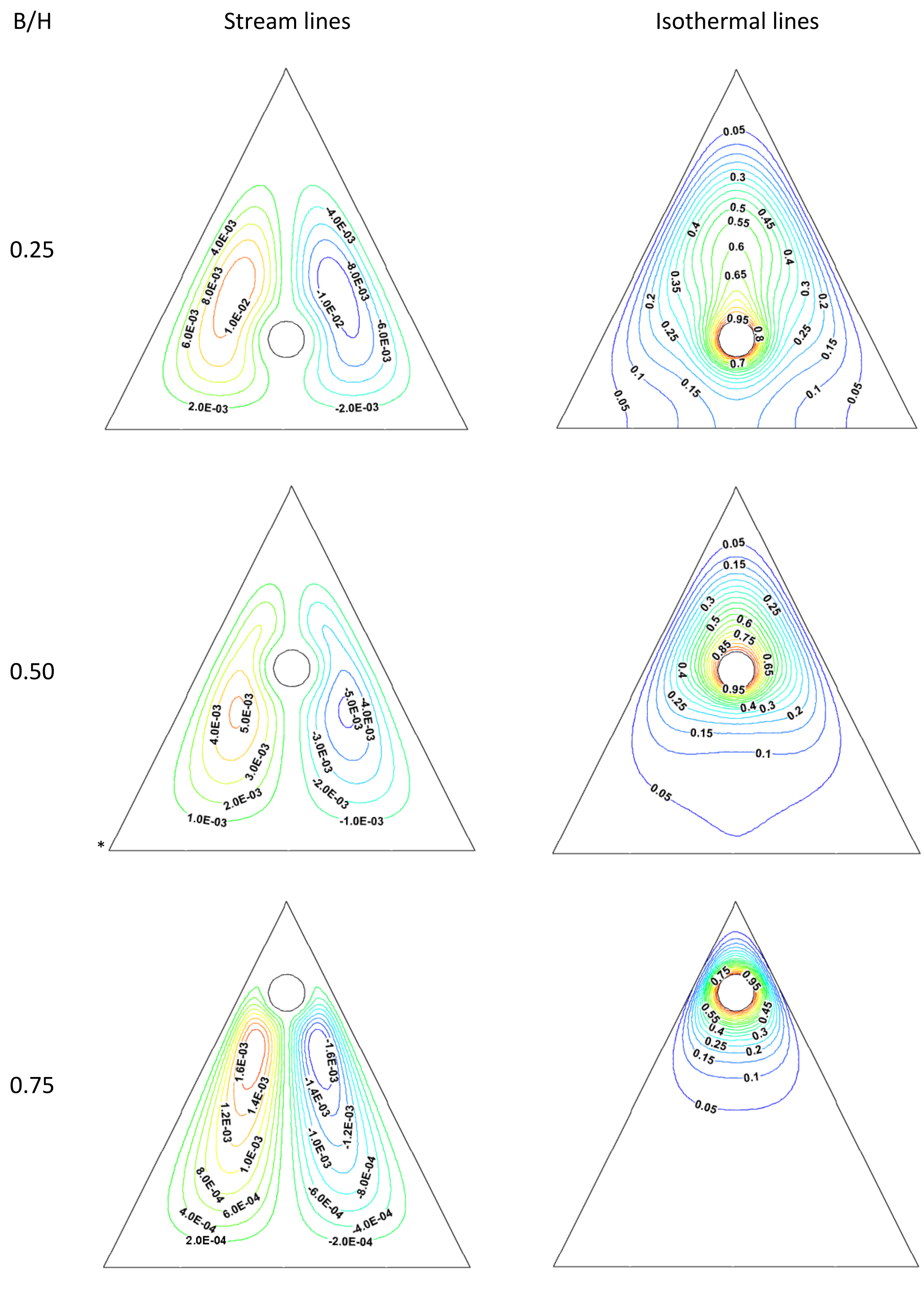


**Fig. 4.** Influence of the position of the source $h$ on the stream lines and the isothermal lines for $Ra=10^5$ and $\phi=0.05$

The influence of the size of the source on the hydrothermal lines for the volume concentration of nanofluid $\phi=0.05$ and for a source positioned at the height of $B=0.25H$ is given in Fig. 5. We note that for $Ra=10^6$, the recirculation velocity for the two sizes are identical, on the other hand, for $Ra=10^3$ the recirculation velocity is higher for the size of the cylinder source $D=0.05L$ by a source size ratio of $D=0.1L$. For the appearance of the isothermal lines, the distribution of heat supplied by the source for the two cases is almost identical.

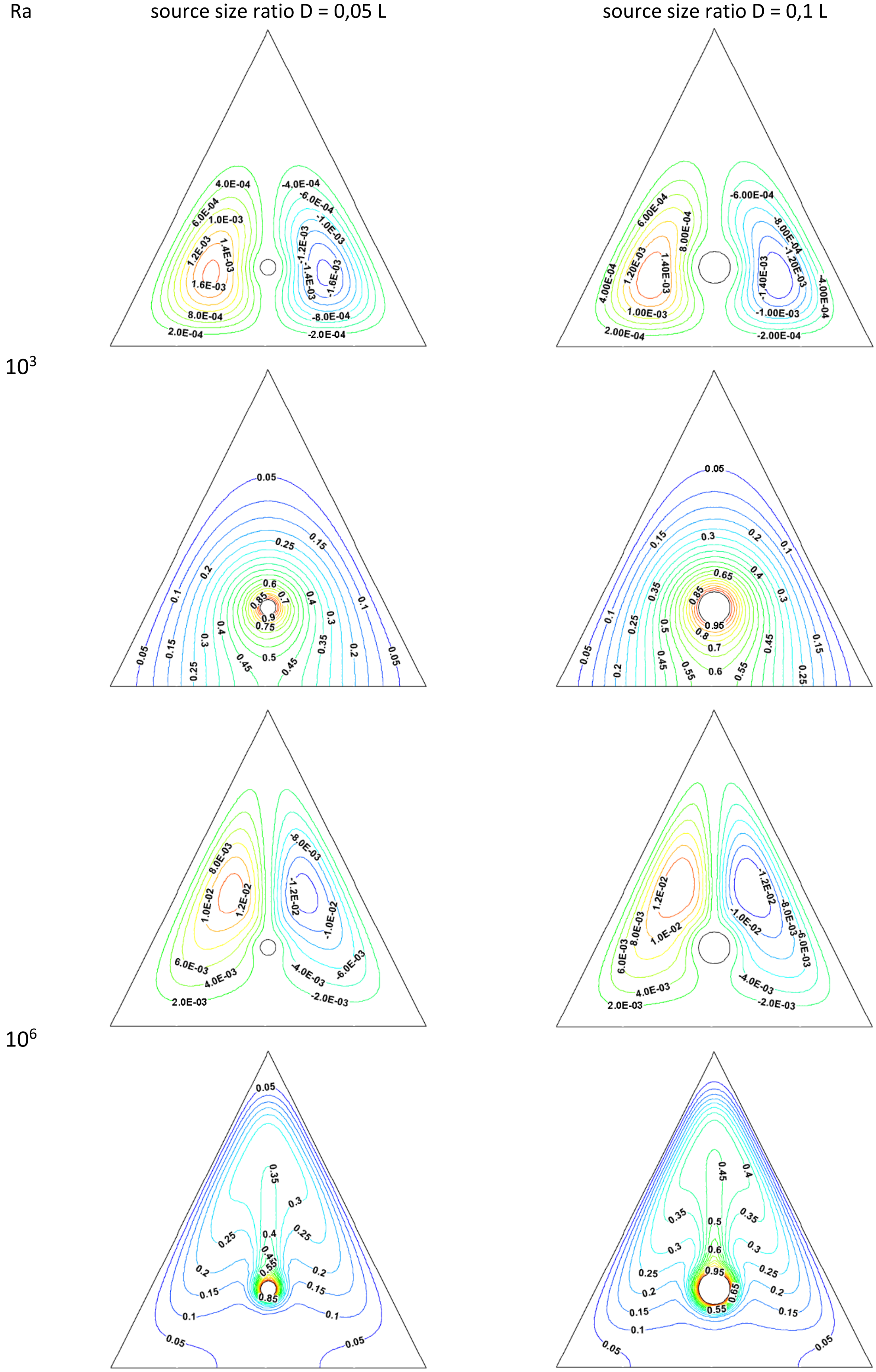


**Fig. 5.** Influence of source size on stream lines and isothermal lines for $\phi$=0.05 and $B$=0.25H

### 4.2 Changes in Nusselt

The aim of this study is to investigate is to inspect the influence of the volume concentration of nanofluid $\phi$, the heat source position B, and $Ra$ on the improvement of convective thermal exchange. Fig. 6 represents the impact of the volumetric concentration of nanofluid on the average values of $Nu$ and for various amounts of $Ra$. The impact of the volume concentration $\phi$ is proportional to the average amounts of $Nu$. In addition, $Nu$ augments with increased volume fraction.

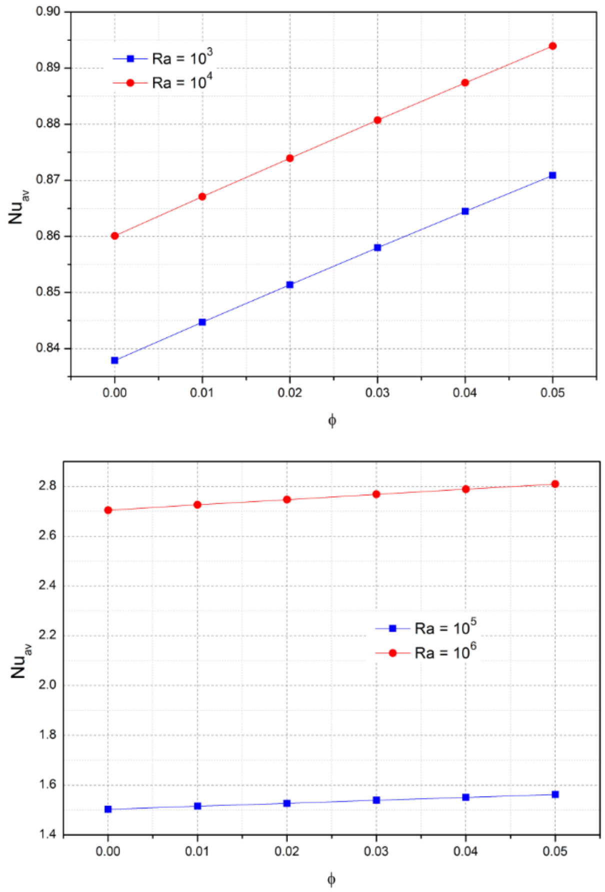


**Fig. 6.** Effect of nanofluid volume concentration on the average Nusselt number for $B$=0.25H and source diameter $D$=0.1L

For $\phi$=0.05, the changes in the average values of $Nu$ vs. Rayleigh number are presented in Fig. 7. As plotted, the impact of $Ra$ on the average $Nu$ is negligible, as long as $Ra$<$10^5$, assisting in this case with the thermal exchange in the conduction mode. For $Ra$>$10^5$, the thermal exchange in the convection mode then takes over, leading to a notable increase in $Nu$.

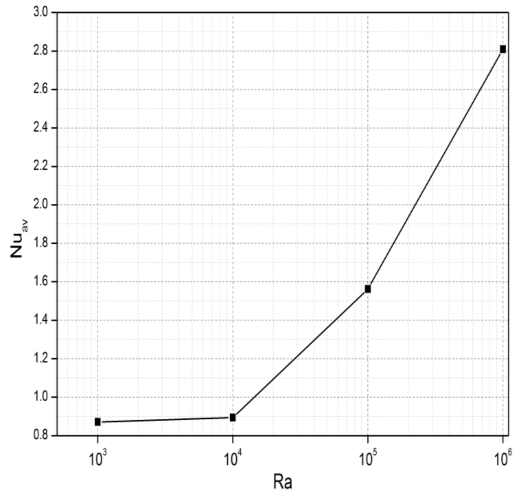


**Fig. 7.** Variation of the average Nusselt number as a function of the Rayleigh number Ra for $\phi$=0.05, $B$=0.25 H and source diameter $D$=0.1 L

Concerning the impact of the source position on the average amounts of Nusselt numbers is illustrated in Fig. 8, we can divide into two parts:

- If the Rayleigh number is less than $10^5$, the closer the cold-walled source gets the average Nusselt number increases. This validates that the thermal exchange is significant for $Ra$<$10^5$ in the conduction mode.
- If the Rayleigh number is greater than $10^5$, the further away from the source with the cold sides, the average Nusselt number increases. This validates that, the heat transfer assistant for $Ra$>$10^5$ in convection mode.

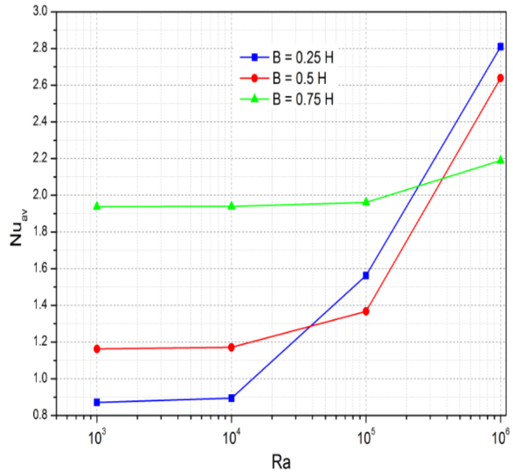


**Fig. 8.** Effect of source position on mean Nusselt number for $\phi$=0.05 and source diameter $D$=0.1L

Fig. 9 reveals the effect of the size of the source positioned at the height of $B$=0.25H on the average amounts of $Nu$ and for the nanofluid concentration $\phi$=0.05. It is noted that is necessary to increase the source diameter for a significant improvement in the thermal exchange.

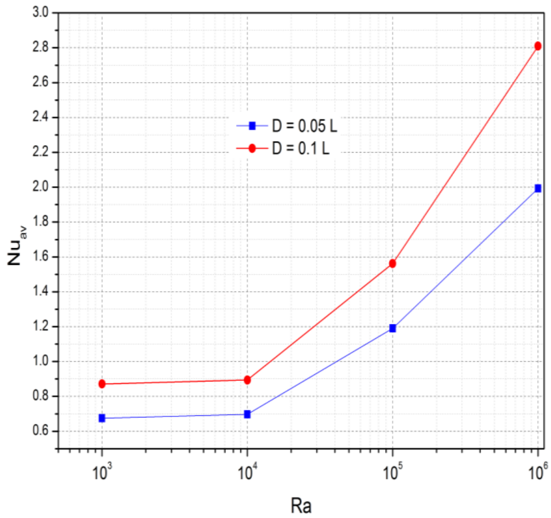


**Fig. 9.** Effect of source size on mean Nusselt number and for $\phi$=0.05

## 4. CONCLUSION

This work performed a computational simulation of convection in a triangular enclosure subjected to thermal and kinematic boundary conditions. The study investigated the influence of the Rayleigh number (*Ra*), nanofluid concentration ($\phi$), and heat source position on the flow field and thermal exchange and explored different values of these three parameters.

- Thermal exchange increases with higher Rayleigh number (*Ra*), source diameter (*D*), and nanofluid volume concentration ($\phi$).
- Heat transfer occurs primarily through conduction for Rayleigh numbers less than $10^5$ and through convection for Rayleigh numbers greater than $10^5$.
- For $Ra<10^5$, heat transfer is more effective when the heat source is closer to the cold walls.
- For $Ra>10^5$, heat transfer is more effective when the heat source is farther from the cold walls.

### Conflicts of Interest

The authors declare no conflict of interest.

## REFERENCES

[1] K.V. Wong O. De Leon, Applications of nanofluids: current and future. *Advances in Mechanical Engineering*, 2, 2010: 519659. https://doi.org/10.1155/2010/519659

[2] Y. Xuan, Q. Li, Heat transfer enhancement of nanofluids. *International Journal of Heat and Fluid Flow*, 21(1), 2000: 58-64. https://doi.org/10.1016/S0142-727X(99)00067-3

[3] Y. Xuan, Q. Li, Investigation on convective heat transfer and flow features of nanofluids. *ASME Journal Heat and Mass Transfer*, 125(1), 2003: 151-155. https://doi.org/10.1115/1.1532008

[4] N. Putra, W. Roetzel, S.K. Das, Natural convection of nano-fluids. *Heat and Mass Transfer*, 39(8), 2003: 775-784. https://doi.org/10.1007/s00231-002-0382-z

[5] V. Bianco, F. Chiacchio, O. Manca, S. Nardini, Numerical investigation of nanofluids forced convection in circular tubes. *Applied Thermal Engineering*, 29(17-18), 2009: 3632-3642. https://doi.org/10.1016/j.applthermaleng.2009.06.019

[6] K. Khanafer, K. Vafai, M. Lightstone, Buoyancy-driven heat transfer enhancement in a two-dimensional enclosure utilizing nanofluids. *International Journal of Heat and Mass Transfer*, 46(19), 2003: 3639-3653. https://doi.org/10.1016/S0017-9310(03)00156-X

[7] M. Shafahi, V. Bianco, K. Vafai, O. Manca, Thermal performance of flat-shaped heat pipes using nanofluids. *International Journal of Heat and Mass Transfer*, 53(7-8), 2010: 1438-1445. https://doi.org/10.1016/j.ijheatmasstransfer.2009.12.007

[8] N.Z. Khan, S. Bilal, L. Kolsi, A.S. Shflot, M.Y. Malik, A case study on entropy generation in MHD nanofluid flow in L-shaped triangular corrugated permeable enclosure. *Case Studies in Thermal Engineering*, 59, 2024: 104487. https://doi.org/10.1016/j.csite.2024.104487

[9] J.A. Eastman, S.U.S. Choi, S. Li, W. Yu, L.J. Thompson, Anomalously increased effective thermal conductivities of ethylene glycol-based nanofluids containing copper nanoparticles. *Applied Physics Letter*, 78(6), 2001: 718-720. https://doi.org/10.1063/1.1341218

[10] S. Lee, S.-S. Choi, Li, J.A. Eastman, Measuring thermal conductivity of fluids containing oxide nanoparticles. *ASME Journal Heat and Mass Transfer*, 121(2), 1999: 280-289. https://doi.org/10.1115/1.2825978

[11] S.P. Jang S.U.S. Choi, Role of Brownian motion in the enhanced thermal conductivity of nanofluids. *Applied Physics Letter*, 84(21), 2004: 4316-4318. https://doi.org/10.1063/1.1756684

[12] S.-E. Ouyahia, K. B. Youb, W. Berabou, M. Benzema, A. Boudiaf, Convection naturelle d'un nanofluide confiné dans une enceinte triangulaire: Effet du fractionnement et de la position de la source de chaleur. *CFM 2017 - 23ème Congrès Français de Mécanique*, August 2017, Lille, France, hal-03465338. (in French)

[13] M.S. Khan, S. Ahmad, Z. Shah, N. Vrinceanu, M.H. Alshehri, Natural convection heat transfer of a hybrid nanofluid in a permeable quadrantal enclosure with heat generation. *Case Studies in Thermal Engineering,* 56, 2024: 104207. https://doi.org/10.1016/j.csite.2024.104207

[14] B. Ghasemi S M. Aminossadati, Brownian motion of nanoparticles in a triangular enclosure with natural convection. *International Journal of Thermal Sciences*, 49(6), 2010: 931-940. https://doi.org/10.1016/j.ijthermalsci.2009.12.017

[15] B. Boudjeniba, A. Laouer, S. Laouar, E.H. Mezaache, Transition to Chaotic Natural Convection of Cu-water Nanofluid in an Inclined Square Enclosure. *International Journal of Heat and Technology*, 37(2), 2019: 413-422. https://doi.org/10.18280/ijht.370206

[16] H.F. Oztop, E. Abu-Nada, Numerical study of natural convection in partially heated rectangular enclosures filled with nanofluids. *International Journal of Heat and Fluid* Flow, 29(5), 2008: 1326-1336. https://doi.org/10.1016/j.ijheatfluidflow.2008.04.009

[17] N. Vedavathi, K. Venkatadri, S. Fazuruddin, G. S.S. Raju, Natural convection flow in semi-trapezoidal porous enclosure filled with alumina-water nanofluid using Tiwari and Das' nanofluid model. *Engineering Transactions,* 70(4), 2022: 303-318. https://doi.org/10.24423/EngTrans.1285.20221004

[18] M. S. Saleh, S. Mekroussi, S. Kherris, D. Zebbar, N. Belghar, A numerical investigation of the effect of sinusoidal temperature on mixed convection flow in a cavity filled with a nanofluid with moving vertical walls. *Heat Transfer*, 52(1), 2022: 7-27. https://doi.org/10.1002/htj.22683

[19] B. Abbou, S. Mekroussi, H. Ameur, S. Kherris, Effect of aspect ratio and nonuniform temperature on mixed convection in a double lid-driven cavity. *Numerical Heat Transfer, Part A: Applications*, 83(8), 2022: 237-247. https://doi.org/10.1080/10407782.2022.2091365

[20] L. Saidi, S. Mekroussi, S. Kherris, D. Zebbar, B. Mébarki, A Numerical Investigation of the Free Flow in a Square Porous Cavity with Non-Uniform Heating on the Lower Wall. *Engineering, Technology & Applied Science Research*, 12(1), 2022: 7982-7987. https://doi.org/10.48084/etasr.4604

[21] C.H. Maatki, K. Ghachem, L. Kolsi, N. Borjini, H. Ben Aissia, Entropy generation of double diffusive natural convection in a three dimensional differentially heated enclosure. *International Journal of Engineering*, 27(2), 2014: 215-226.

[22] K. Ghachem, W. Hassen, C. Maatki, L. Kolsi, A. A. Al-Rashed, M. Naceur, Numerical simulation of 3D natural convection and entropy generation in a cubic cavity equipped with an adiabatic baffle. *International Journal of Heat and Technology*, 36(3), 2018: 1047-1054. https://doi.org/10.18280/ijht.360335

[23] A.S. Dogonchi, A.J. Chamkha, D.D. Ganji, A numerical investigation of magnetohydrodynamic natural convection of Cu–water nanofluid in a wavy cavity using CVFEM. *Journal of Thermal Analysis and Calorimetry*, 135, 2019: 2599-2611. https://doi.org/10.1007/s10973-018-7339-z

[24] M. Hashemi-Tilehnoee, A.S. Dogonchi, S.M. Seyyedi, A.J. Chamkha, D.D. Ganji, Magnetohydrodynamic natural convection and entropy generation analyses inside a nanofluid-filled incinerator-shaped porous cavity with wavy heater block. *Journal of Thermal Analysis and Calorimetry*, 141, 2020: 2033-2045. https://doi.org/10.1007/s10973-019-09220-6

[25] T. Tayebi A. J. Chamkha, Magnetohydrodynamic natural convection heat transfer of hybrid nanofluid in a square enclosure in the presence of a wavy circular conductive cylinder. *Journal of Thermal Science and Engineering Applications*, 12(3), 2020: 031009. https://doi.org/10.1115/1.4044857

[26] K. Khanafer K. Vafai, A critical synthesis of thermophysical characteristics of nanofluids. *International Journal of Heat and Mass Transfer*, 54(19-20), 2011: 4410-4428.

https://doi.org/10.1016/j.ijheatmasstransfer.2011.04.048

[27] T. Hayase, J.A.C. Humphrey, R. Greif, A consistently formulated QUICK scheme for fast and stable convergence using finite-volume iterative calculation procedures. *Journal of Computational Physics*, 98(1), 1992: 108-118. https://doi.org/10.1016/0021-9991(92)90177-Z

[28] A. Arefmanesh, M. Amini, M. Mahmoodi, M. Najafi, Buoyancy-driven heat transfer analysis in two-square duct annuli filled with a nanofluid. *European Journal of Mechanics - B/Fluid,* 33, 2012: 95-104. https://doi.org/10.1016/j.euromechflu.2011.11.004